IET Smart Grid

Research Article

IET Journals
The Institution of Engineering and Technology

Rebound behaviour of uncoordinated EMS and their impact minimisation

eISSN 2515-2947
Received on 17th June 2019
Revised 17th October 2019
Accepted on 25th November 2019
E-First on 4th February 2020
doi: 10.1049/iet-stg.2019.0158
www.ietdl.org

Khizir Mahmud[1] ✉, *Jayashri Ravishankar*[1], *Jahangir Hossain*[2]

[1]*School of Electrical Engineering and Telecommunications, University of New South Wales, NSW 2052, Australia*
[2]*School of Engineering, Macquarie University, NSW 2109, Australia*
✉ *E-mail: khizir.mahmud@unsw.edu.au*

Abstract: In this paper, the impacts of uncoordinated energy management systems (EMS), with a rebound effect, on a renewable energy-dependent microgrid are discussed and feasible solutions are presented. Two different approaches, i.e. load-based and price-based EMS are modelled which consider PV units, battery energy storage systems (BESS), and electric vehicles (EVs). Taking account of each component's boundary conditions, the load-based approach intelligently charges the EV and BESS from the grid/PV during off-peak hours, and provides a combined discharge response during peak load hours. In the price-based approach, the charging-discharging of BESSs and EVs from/to grid and PV depends on the time-of-use tariff signal. The primary objective of both models is to minimise the customers' peak electricity consumption and the saturation issues of distribution transformers. It is observed that the simultaneous response of the EMS due to the identical behaviour of load or price curves, and the rebound effect after mode switching transition create large power demand spikes. To mitigate its negative consequence, an improved locking and randomisation technique is designed and implemented. Additionally, the impact of the PV power fluctuations on the load-support systems due to fast-moving clouds and their consequences to the behaviour of the EMS response are investigated.

Nomenclature

$t^j_{\mathbb{B}}$, $t^j_{\mathscr{P}}$	off-peak and peak load periods, respectively
$\mathfrak{D}^t_{\mathbb{D}}$	customer's desired (reference) power demand
$\mathfrak{C}^t_{\mathbb{P}}$	electricity cost curve
λ^l_{ev}, λ^l_{b}	minimum discharging limit of EV and battery, respectively
λ^i_{ev}, λ^i_{b}	current SOC of EV and battery, respectively
β^c_{ev}, β^c_{b}	capacity of EV battery and BESS, respectively
λ^i_{pv}	instantaneous PV power generation

1 Introduction

The conventional power system has undergone a substantial change in last decades which has led to a fundamental shift in the traditional generation and management of electrical energy [1–3]. In recent years, small-scale renewable energy generators supersede the bulky large-scale generators. The electricity is now generated close to the customer premises from distributed generators including rooftop photovoltaics (PVs), or aggregated PVs and wind generators. Various centralised and decentralised control approaches are used to manage these distributed and non-dispatchable renewable generators. As renewable energy sources are intermittent, the uninterrupted power supply by regulating voltage and frequency remains a major challenge [1–3].

Energy storage deployment either at home or grid side is a standard solution to mitigate intermittency issues. It stores excess energy from the renewables during off-peak hours in the middle of a day, and discharges during peak hours or in the absence of renewable energy generation. Another form of battery storage is the electric vehicle (EV) that is becoming popular due to its bidirectional vehicle-to-grid (V2G) energy transfer mechanism [1, 2]. The charging–discharging mechanisms of the battery in an EV are similar to that of a stationary battery; however, the mobility makes these significantly complex. Therefore, to mitigate intermittency through intermittent storage (i.e. EVs, due to its mobility), an extra level of management and their charge scheduling is necessary. The battery-to-grid and V2G facilitate prosumers to participate in both local and global energy markets, or the wholesale energy market through aggregated EVs [1, 3]. Additionally, various embedded devices and energy management systems (EMS) are used at the domestic level to enhance energy efficiency and utilise it to participate in the energy transactions.

Along with EVs, roof-top PV units are also common modes for small-scale local energy generation. However, to a certain extent both resources are intermittent. Therefore, the use of automatic domestic EMS is quite common at a domestic level. Various strategies are adopted in the EMS whose primary objective is to minimise the electricity cost [4]. There are two common strategies adopted in these EMS. One approach is to check the load conditions and schedule the loads or energy resources [5]. Another way is to check the electricity prices and schedule the loads and energy resources [6]. Usually, once the main parameter (load or price signal) is met considering other constraints, all the resources are scheduled accordingly. In this case, any uncoordinated EMS may lead to an unwanted variation in the system parameters.

Numerous studies in the field of microgrid and domestic energy management have focused on the control techniques and components (storages, EVs, PV units). Mahmud *et al*. [7] propose a decision-tree-based algorithm to reduce the domestic peak load using EVs, PV units, and battery storage. The EVs are used in [8] to flatten the fluctuating load profile of a building. It uses roof-top PV units to charge EV battery and any negative consequences by fast charging of EVs are managed. EVs are also utilised to manage the power demand in a medium scale, e.g. university, commercial buildings [4, 9]. In this case, EVs in a parking lot are aggregated and their charging–discharging are scheduled based on the load demand of the consumers. Domestic peak load demand management is studied by authors in [10–12], where an individualised electricity pricing policy [12] and utility-defined prices [10, 11] are proposed to optimally manage the customers' power demand and minimise the peaks in load curves. Other studies [6, 13] investigate the use of V2G to minimise the impact of PVs due to its power generation fluctuations. In most of these PV-related studies, the data acquisition to controller is done in a minute timeframe. However, the impact of sub-second time-scale

fluctuation and the performance of the system remains unclear, as the data granularity in a minute scale may miss the system response that is happening in sub-second scale.

The grid-level placement of storages (aggregated EVs, battery storage) are investigated in [14]. In this case, the impact of intermittent power generators on individual domestic systems under a substation are not well addressed. Therefore, some researchers [15, 16] focused on analysing the voltage and frequency deviation by intermittent renewable energy sources at a domestic level. A study in [17] investigates the rebound effect of the energy storages under an EMS. Another study [18] analysed the behaviour of rebound effect of demand response during frequency restoration and systems efficiency [19]. However, the rebound effect of the storage devices during PV-power-generation fluctuating condition and their overall impact on the microgrid substation needs to be further analysed. In some analysis, a combination of battery energy storage systems (BESSs) and intermittent EVs are proposed to minimise the uncertainty of weather-dependent loads and sources [20, 21]. Most of the energy management approaches that deals with the integration of renewable energy sources and energy storages consider a single control layer, i.e. either primary, secondary, or tertiary layer. Thus, the performance of the EMS considering the holistic impact remains unclear.

A comprehensive study in [22] analyses the strategic deployment of EVs in a microgrid to provide load and power quality support. However, a holistic impact by different types of load patterns and their behaviours to the EMS are needed to be further investigated. Another common method to tackle the load demand of a grid-connected or islanded microgrid is to shift the controllable loads [23] and minimise the peaks [24] either in real-time [25] or day-ahead operation [26]. In some investigations [27], AC/DC hybrid microgrid considering various intermittent renewable energy sources are discussed. These hybrid microgrid-related studies present voltage and frequency control strategies [27], power transfer operation [28], and dynamic power management [29].

Although extensive research has been carried out on various type of EMS in a microgrid, very little attention was paid to investigate the impact of uncoordinated EMS with rebound effect on the performance of a microgrid. Considering previous studies, the importance and originality of this study are to analyse and explore:

- the two different types of EMS, i.e. load-based and price-based EMS, and their rebound effect on the heavily renewable energy-dependent distribution systems,
- the effect of PV power fluctuations by fast-moving clouds on the individual EMS and in the substation,
- the rebound effect of an individual EMS due to PV power fluctuations and their impact at the substation,
- the characteristics of the uncoordinated EMS and their identical behavioural effects to the grid, and a solution to minimise the negative consequences.

The rest of the paper is organised as follows. Section 2 provided an overview of the problem and the system architecture. The problem is formulated along with EMS algorithm in Section 3. Various case studies are conducted in Section 4 with the following conclusion in Section 5.

2 Problem overview and motivation

A domestic EMS is modelled to investigate its impact on uncoordinated states. It considers two different approaches, e.g. load-based and price-based. The main objective in these two approaches is to minimise the cost and avoid the over-saturation of distribution transformer. The system consists of a BESS, a EV, and PV units. In the load-based approach, the charge management of the BESS and EV is performed during the off-peak hours and discharge during the peak hours to minimise the electricity cost. Moreover, these storages utilise the excess energy from the PV unit to charge during off-peak hours. In this EMS, battery's and EV's state-of-charge (SOC), EV availability, EV trip plan, PV power generation, load conditions, and so on are the constraints. Although renewable energy generation curves, in particular, weather zone and geographical location follow similar pattern, the power demand for every household at a particular time might not be the same. It is because every household does not have the same appliances and same operation times. However, the PV power generation is dependent on weather, and thus it changes its output at the same time for a particular region. For example, if there is any cloud passing through quickly, the output of PVs will fluctuate quickly. Any houses highly dependent on the roof-top PV units will experience this fluctuation which will trigger all the load-based EMS to execute a certain function at the same time. In this case, rebound effects can create unwanted oscillations in the system.

On the other hand, in price-based approach the electricity cost is considered as a main factor to manage the charging–discharging of the battery storage and EVs. Usually, battery storages and EVs are charged when energy cost is lower and discharge when energy price is higher. In this approach, the common constraints such as SOC of the battery and EV, EV availability, EV trip plan, PV power generation and load conditions are considered. In some energy market (e.g. Australia), wholesale energy price changes every 5 min, and 30 min, sometimes with a high fluctuation [30]. Similar to the load-based approach, this fluctuation in price may trigger all the price-based EMS to execute a specific function at particular time. Thus, any rebounding effect can create oscillations in the system.

In case of the load-based energy management approach, the EMS trigger its charging and discharging switch considering the off-peak and peak load conditions. For example, if the load demand suddenly drops (i.e. becomes off-peak), the EMS triggers the battery storage and EV charging. If all the EMS functions under the same approach, in a small network, the load demand immediately after becoming off-peak may experience extra load demand or spikes due to the charging of battery storage and EVs. The same scenario may happen for the price-based EMS as well. In this paper, this effect is considered as rebound effect. The effect motivates to investigate its impact on a small network under various EMS approaches.

A detailed architecture of the proposed model and their uncoordinated deployment among customers is shown in Fig. 1. All the domestic loads, EV, and energy resources are connected to a common AC bus. The battery storage and PV are connected to an intermediate DC bus. A PV unit is connected to the DC bus through a DC–DC converter. A battery is connected to the DC bus through a bidirectional DC–DC converter. This DC bus is connected to the AC bus through a bidirectional DC–AC/AC–DC converter. The EV is connected to the AC bus through a bidirectional DC–AC/AC–DC converter. A controller collects load-demand data, battery and EV SOC, EV availability, and PV power-generation data. Based on this data and the predefined algorithm, the controller controls the inverters, i.e. the power flow from/to the AC/DC buses and storages.

3 EMS algorithms and problem formulation

The domestic load demand [4, 7, 13, 31] can be expressed as a function of power and time as follows:

$$\mathcal{S}_{\mathbb{P}}^{t} = f\left(\mathscr{P}, t_{\ell}^{j}\right) \tag{1}$$

The time (t_{ℓ}^{j}) in the load demand function is the summation of both off-peak $\left(t_{\mathbb{B}}^{j}\right)$ and peak load periods $\left(t_{\mathscr{P}}^{j}\right)$ as follows:

$$t_{\ell}^{j} = \left(t_{p}^{j} \cup t_{b}^{j}\right) \tag{2}$$

$$t_{\mathscr{P}}^{j} = \mathcal{O}_{\mathscr{P}}^{f} * \sum_{j=0}^{n} t_{\mathscr{P}}^{j} \tag{3}$$

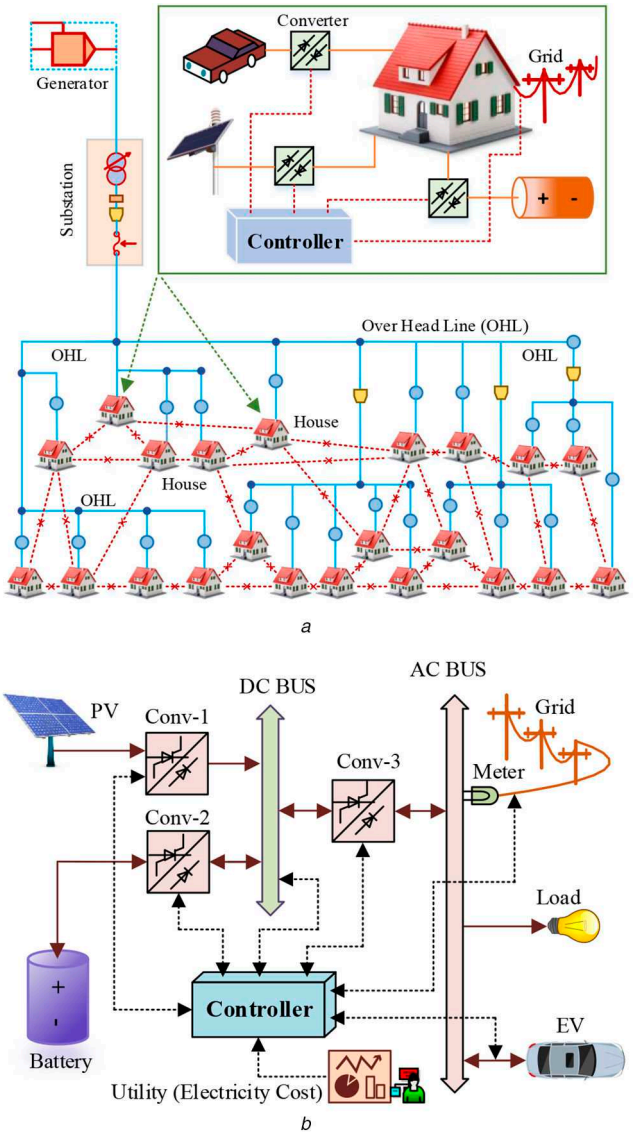

Fig. 1 *EMS architecture and their deployment across the power distribution systems*

(a) Basic schematic of the proposed EMS and their uncoordinated deployment across the power distribution systems, ***(b)*** Detailed layout of the EMS

$$t_{\mathbb{B}}^{j} = \mathcal{O}_{\mathbb{B}}^{f} * \sum_{j=0}^{n} t_{\mathbb{B}}^{j} \tag{4}$$

where $t_{\mathscr{P}}^{0}$ and $t_{\mathscr{P}}^{n}$ are the initial and final time of the peak load occurrence periods, respectively. Similarly, $t_{\mathbb{B}}^{0}$ and $t_{\mathbb{B}}^{n}$ are the initial and final times of the off-peak load (base load) periods, respectively. $\mathcal{O}_{\mathscr{P}}^{f}$ and $\mathcal{O}_{\mathbb{B}}^{f}$ are the peak and off-peak load occurrence frequency for a particular time duration, respectively. The load data acquisition rate to the controller is as follows:

$$\text{data rate}\begin{cases}\left(t_{\mathscr{P}}^{1} - t_{\mathscr{P}}^{0}\right)\\ \left(t_{\mathbb{B}}^{1} - t_{\mathbb{B}}^{0}\right)\end{cases} \tag{5}$$

For a load-based EMS, the customer's desired power demand curve is assumed as

$$\mathfrak{D}_{\mathbb{D}}^{t} = f\left(\mathscr{P}_{\partial}, t_{\ell}^{j}\right) \tag{6}$$

For price-based EMS, the electricity cost curve $\left(\mathfrak{S}_{\mathbb{P}}^{t}\right)$ is a function of electricity price and time as follows:

$$\mathfrak{S}_{\mathbb{P}}^{t} = f\left(\mathscr{C}_{e}, t_{\ell}^{j}\right) \tag{7}$$

$$\mathfrak{S}_{d}^{t} = f\left(\mathscr{C}_{r}, t_{\ell}^{j}\right)d \tag{8}$$

where $\mathscr{C}_{e}$ is the electricity price, $\mathscr{C}_{r}$ is the reference electricity price, and $\mathfrak{S}_{\mathbb{D}}^{t}$ is the reference electricity cost curve to define peak and off-peak load periods. The peak and off-peak load is identified by the following relation:

$$\begin{aligned}&\text{peak load}\left\{\mathcal{S}_{\mathbb{P}}^{t} > \mathfrak{D}_{\mathbb{D}}^{t}, \mathfrak{S}_{\mathbb{P}}^{t} > \mathfrak{S}_{d}^{t}\right.\\ &\text{off}-\text{peak load}\left\{\mathcal{S}_{\mathbb{P}}^{t} < \mathfrak{D}_{\mathbb{D}}^{t},\ \mathfrak{S}_{\mathbb{P}}^{t} < \mathfrak{S}_{d}^{t}\right.\end{aligned} \tag{9}$$

For the houses with the roof-top PV units, the desired reference curve $\left(\mathfrak{D}_{\mathbb{D}}^{t}\right)$ in (6) can be set above the maximum power generation capacity of those PVs.

The currents from the EV and battery are denoted as $i_{\text{ev}}^{t_1}, i_{\text{ev}}^{t_2}, i_{\text{ev}}^{t_3}, \ldots, i_{\text{ev}}^{t_n}$ and $i_{\text{b}}^{t_1}, i_{\text{b}}^{t_2}, i_{\text{b}}^{t_3}, \ldots, i_{\text{b}}^{t_n}$, respectively. The sign of this current will identify the charging and discharging modes of the battery and EV, i.e.

$$\begin{aligned}&i_{\text{b}}^{t}, i_{\text{ev}}^{t} < 0 \rightarrow \text{battery and EV charging}\\ &i_{\text{b}}^{t}, i_{\text{ev}}^{t} > 0 \rightarrow \text{battery and EV discharging}\end{aligned} \tag{10}$$

If the instantaneous power demand at a particular time is $\mathcal{S}_{\mathbb{P}}^{t_1}$ and $\mathcal{S}_{\mathbb{P}}^{t_1} > \mathfrak{D}_{\mathbb{D}}^{t}$, then, the amount of power required to shave the peak load is

$$\mathcal{S}_{\mathbb{P}}^{s} = \mathcal{S}_{\mathbb{P}}^{t_1} - \mathfrak{D}_{\mathbb{D}}^{t}, \quad \text{for} \quad \mathcal{S}_{\mathbb{P}}^{t} > \mathfrak{D}_{\mathbb{D}}^{t},\ \mathfrak{S}_{\mathbb{P}}^{t} > \mathfrak{S}_{d}^{t} \tag{11}$$

This power will be provided by the battery, PV, and EV depending on their availability and discharging constraints.

If the instantaneous power demand at a particular time is $\mathcal{S}_{\mathbb{P}}^{t_1} < \mathfrak{D}_{\mathbb{D}}^{t}$, the available power to charge the EV and battery is

$$\mathcal{S}_{\mathbb{P}}^{c} = \mathfrak{D}_{\mathbb{D}}^{t} - \mathcal{S}_{\mathbb{P}}^{t_1}, \quad \text{for} \quad \mathcal{S}_{\mathbb{P}}^{t} < \mathfrak{D}_{\mathbb{D}}^{t}, \mathfrak{S}_{\mathbb{P}}^{t} < \mathfrak{S}_{d}^{t} \tag{12}$$

If the minimum limit for the EV and battery SOC (for discharging) is λ_{ev}^{l} and λ_{b}^{l}, respectively, and the current SOC of the EV and battery is λ_{ev}^{i} and λ_{b}^{i}, respectively, the maximum available power that the EV and battery can provide to the required load support $\left(\mathcal{S}_{\mathbb{P}}^{s}\right)$ is

$$\lambda_{\text{b}}^{\text{av}} = \beta_{\text{b}}^{c}\left(\lambda_{\text{b}}^{i} - \lambda_{\text{b}}^{l}\right) \tag{13}$$

$$\lambda_{\text{ev}}^{\text{av}} = \beta_{\text{ev}}^{c}\left(\lambda_{\text{ev}}^{i} - \lambda_{\text{ev}}^{l}\right) \tag{14}$$

Here, β_{ev}^{c} is the battery capacity of EV and β_{b}^{c} is the capacity of the stationary battery. So, the power provided by the PV, EV, and battery to shave $\left(\mathcal{S}_{\mathbb{P}}^{s}\right)$ is as follows:

$$\begin{aligned}\mathcal{S}_{\mathbb{P}}^{s} = &\left\{\lambda_{\text{ev}}^{\text{av}}\left(1 - \text{e}^{-\lambda_{\text{ev}}^{i=t_1, t_1+1, \ldots, t_2}}\right)\right\} + \left\{\lambda_{\text{b}}^{\text{av}}\left(1 - \text{e}^{-\lambda_{\text{b}}^{i=t_1, t_1+1, \ldots, t_2}}\right)\right\}\\ &+ \lambda_{\text{pv}}^{i}\end{aligned} \tag{15}$$

where λ_{pv}^{i} represents the instantaneous PV power generation. If the current charge of the battery and EV is $\lambda_{\text{b}}^{i=t_1, t_1+1, \ldots t_2}$, and $\lambda_{\text{ev}}^{i=t_1, t_1+1, \ldots, t_2}$, respectively, and the maximum charging limit of the battery and EV is λ_{b}^{m} and λ_{ev}^{m}, respectively, the available grid power $\left(\mathcal{S}_{\mathbb{P}}^{c}\right)$ to charge the battery and EV is

$$\begin{aligned}\mathcal{S}_{\mathbb{P}}^{c} = &\left\{\lambda_{\text{ev}}^{r}\left(\text{e}^{(1/(-\lambda_{\text{ev}}^{i=t_1, t_1+1, \ldots, t_2}))}\right)\right\} + \left\{\lambda_{\text{b}}^{r}\left(\text{e}^{(1/(-\lambda_{\text{b}}^{i=t_1, t_1+1, \ldots t_2}))}\right)\right\}\\ &\text{for} \quad \mathcal{S}_{\mathbb{P}}^{t} < \mathfrak{D}_{\mathbb{D}}^{t}, \mathfrak{S}_{\mathbb{P}}^{t} < \mathfrak{S}_{d}^{t}\end{aligned} \tag{16}$$

$$\lambda_{\text{ev}}^{r} = \beta_{\text{ev}}^{c}\left(\lambda_{\text{ev}}^{m} - \lambda_{\text{ev}}^{i}\right) \tag{17}$$

$$\lambda_{\text{b}}^{r} = \beta_{\text{b}}^{c}\left(\lambda_{\text{b}}^{m} - \lambda_{\text{b}}^{i}\right) \tag{18}$$

The PV power is utilised to provide the peak load support and a portion is used to charge the battery. The PV power supply to the DC bus through converter 1 is

$$\lambda_{\text{pv}}^{i} = n \cdot \gamma_{\text{pv}}^{g} \cdot \eta_{1} \quad \text{for} \quad \mathcal{S}_{\mathbb{P}}^{t} = \lambda_{\text{pv}}^{i} \tag{19}$$

where γ_{pv}^{g} represents the PV power generation from a single cell, n represents the number of cells, η_1 represents the efficiency of the converter 2. For $\mathcal{S}_{\mathbb{P}}^{t} > \lambda_{\text{pv}}^{i}$, the excess energy is supplied by the EV and battery.

In case of $\mathcal{S}_{\mathbb{P}}^{t} < \lambda_{\text{pv}}^{i}$, PV has excess energy after supplying the load demand. So, this excess energy is bypassed to the battery through converter 2, and is given as

$$\xi_{\text{ex}}^{\text{pv}} = \begin{cases} 0 & \text{when } \mathcal{S}_{\mathbb{P}}^{t} \geq \lambda_{\text{pv}}^{i},\ i \in t_{\ell}^{j} \\ \lambda_{\text{pv}}^{i} - \mathcal{S}_{\mathbb{P}}^{t} & \text{when } \mathcal{S}_{\mathbb{P}}^{t} < \lambda_{\text{pv}}^{i},\ i \in t_{\ell}^{j} \end{cases} \tag{20}$$

For $\mathcal{S}_{\mathbb{P}}^{t} > \lambda_{\text{pv}}^{i}$, the excess energy to support the load is supplied by the EV and battery. The cost of electricity in this charging and discharging process is

$$\left\{\Delta_{e}^{b} * f\left(\mathscr{P}, t_{b}^{j}\right)\right\} + \left\{\Delta_{e}^{p} * \left(f\left(\mathscr{P}, t_{\mathbb{P}}^{j}\right)\right)\right\} \tag{21}$$

where Δ_e^p and Δ_e^b are the electricity cost during peak and off-peak load hours, respectively. In case of excess power generation by the renewables and battery storage, and the house does not have a provision to penetrate power back to grid, the system constraints will be

$$\mathcal{S}_{\mathbb{P}}^{t} - \mathfrak{D}_{\mathbb{D}}^{t} \geq 0 \quad \text{for} \quad t_{\ell}^{j} \tag{22}$$

$$\lambda_{\text{b}}^{l} < \lambda_{\text{b}}^{i} < \lambda_{\text{b}}^{m} \tag{23}$$

$$\lambda_{\text{ev}}^{l} < \lambda_{\text{ev}}^{i} < \lambda_{\text{ev}}^{m} \tag{24}$$

Both the load-based and price-based algorithms are described in Algorithms 1 and 2 (see Figs. 2 and 3), respectively. The battery and EV charging–discharging algorithm, and boundary conditions are shown in Figs. 4*a* and *b*.

As the trip of EVs are highly uncertain, the battery SOC of the EV is segmented into five parts: $\mathcal{S}_0, \mathcal{S}_1, \mathcal{S}_2, \mathcal{S}_3, \mathcal{S}_4$. The segment $\mathcal{S}_0$ is utilised to provide the emergency trip support and the battery capacity must not drop below this limit. EV battery will charge rapidly in this stage of SOC. For the $\mathcal{S}_1$ SOC stage, EV will also charge rapidly if the owner has a long trip plan. The battery will charge flexibly based on the load conditions in the $\mathcal{S}_2$ stage. The battery will discharge based on the load conditions in $\mathcal{S}_3$ stage. $\mathcal{S}_4$ is the maximum battery charging limit. To maximise the battery life, the battery constraints are

$$\mathcal{S}_0 \geq \text{emergency reserve} \tag{25}$$

$$\mathcal{S}_4 \leq 100\%\text{SOC} \tag{26}$$

The value of the segments can be set based on the SOC and mileage process. The following scenario may occur in the charge scheduling process.

Scenario 1

$\left(\lambda_{\text{ev}}^{i} < \mathcal{S}_1 \text{ for } \mathcal{S}_{\mathbb{P}}^{t} > \mathfrak{D}_{\mathbb{D}}^{t}, \mathcal{S}_{\mathbb{P}}^{t} < \mathfrak{D}_{\mathbb{D}}^{t} \text{ and } \mathfrak{S}_{\mathbb{P}}^{t} > \mathfrak{S}_{\mathbb{D}}^{t}, \mathfrak{S}_{\mathbb{P}}^{t} < \mathfrak{S}_{d}^{t}\right)$ In this case, EV SOC is at $\mathcal{S}_0$, and therefore the charging rate ($\alpha(t)$) is

$$\alpha(t) = \alpha(t)_{\max} \quad \text{for} \quad \lambda_{\text{ev}}^{i} < \mathcal{S}_1 \tag{27}$$

For $\mathcal{S}_{\mathbb{D}}^{t} < \mathfrak{D}_{\mathbb{D}}^{t}$ or $\mathfrak{S}_{\mathbb{D}}^{t} < \mathfrak{S}_{d}^{t}$, the power $\alpha(t)_{\max}$ will be supplied by the grid from $\mathcal{S}_{\mathbb{P}}^{c}$. However, for $\mathcal{S}_{\mathbb{P}}^{t} > \mathfrak{D}_{\mathbb{D}}^{t}$ or $\mathfrak{S}_{\mathbb{P}}^{t} > \mathfrak{S}_{d}^{t}$, the battery and grid will supply the required power ($\alpha(t)_{\max}$).

Scenario 2

$\left(\mathcal{S}_0 < \lambda_{\text{ev}}^{i} < \mathcal{S}_2 \text{ for } \mathcal{S}_{\mathbb{P}}^{t} > \mathfrak{D}_{\mathbb{D}}^{t}, \mathcal{S}_{\mathbb{P}}^{t} < \mathfrak{D}_{\mathbb{D}}^{t} \text{ and } \mathfrak{S}_{\mathbb{P}}^{t} > \mathfrak{S}_{d}^{t}, \mathfrak{S}_{\mathbb{P}}^{t} < \mathfrak{S}_{d}^{t}\right)$

Although $\lambda_{\text{ev}}^{i} > \mathcal{S}_0$, rapid charging is preferable if the owner has a long trip plan. The charging rate is

$$\begin{aligned} \alpha(t) = \alpha(t)_{\max} \quad \text{for} \quad & \mathcal{S}_0 < \lambda_{\text{ev}}^{i} < \mathcal{S}_2, \\ & \mathcal{S}_{\mathbb{P}}^{t} > \mathfrak{D}_{\mathbb{D}}^{t}, \mathfrak{S}_{\mathbb{P}}^{t} > \mathfrak{S}_{d}^{t} \text{ and } \mathcal{S}_{\mathbb{P}}^{t} < \mathfrak{D}_{\mathbb{D}}^{t}, \mathfrak{S}_{\mathbb{P}}^{t} < \mathfrak{S}_{d}^{t} \end{aligned} \tag{28}$$

The flexible EV charging rate based on the load conditions is

$$\mathcal{S}_{\mathbb{P}}^{c} = \underbrace{\left\{\lambda_{\text{ev}}^{r}\left(\text{e}^{(1/(-\lambda_{\text{ev}}^{i=t_1, t_1+1, \ldots, t_2)})}\right)\right\}}_{\alpha(t)} + \underbrace{\left\{\lambda_{\text{b}}^{r}\left(\text{e}^{(1/(-\lambda_{\text{b}}^{i=t_1, t_1+1, \ldots t_2)})}\right)\right\}}_{\text{battery charge rate}} \tag{29}$$

$$\text{for } \mathcal{S}_0 < \lambda_{\text{ev}}^{i} < \mathcal{S}_2, \mathcal{S}_{\mathbb{P}}^{t} < \mathfrak{D}_{\mathbb{D}}^{t}, \mathfrak{S}_{\mathbb{P}}^{t} < \mathfrak{S}_{d}^{t}$$

Scenario 3

$\left(\mathcal{S}_1 < \lambda_{\text{ev}}^{i} < \mathcal{S}_3 \text{ for } \mathcal{S}_{\mathbb{P}}^{t} > \mathfrak{D}_{\mathbb{D}}^{t}, \mathcal{S}_{\mathbb{P}}^{t} < \mathfrak{D}_{\mathbb{D}}^{t} \text{ and } \mathfrak{S}_{\mathbb{P}}^{t} > \mathfrak{S}_{d}^{t}, \mathfrak{S}_{\mathbb{P}}^{t} < \mathfrak{S}_{d}^{t}\right)$

The flexible charging rate is (see (30)) .

Scenario 4

$\left(\mathcal{S}_2 < \lambda_{\text{ev}}^{i} < \mathcal{S}_4 \text{ for } \mathcal{S}_{\mathbb{P}}^{t} > \mathfrak{D}_{\mathbb{D}}^{t}, \mathcal{S}_{\mathbb{P}}^{t} < \mathfrak{D}_{\mathbb{D}}^{t} \text{ and } \mathfrak{S}_{\mathbb{P}}^{t} > \mathfrak{S}_{d}^{t}, \mathfrak{S}_{\mathbb{P}}^{t} < \mathfrak{S}_{d}^{t}\right)$

For $\mathcal{S}_{\mathbb{P}}^{t} > \mathfrak{D}_{\mathbb{D}}^{t}$ or $\mathfrak{S}_{\mathbb{P}}^{t} > \mathfrak{S}_{d}^{t}$, the EV will discharge, and the discharge rate ($\vartheta(t)$) is

$$\begin{aligned} \vartheta(t) &= \left\{\lambda_{\text{ev}}^{\text{av}}\left(1 - \text{e}^{-\lambda_{\text{ev}}^{i=t_1, t_1+1, \ldots, t_2}}\right)\right\} \\ &= \left\{\mathcal{S}_{\mathbb{P}}^{s} - \left\{\lambda_{\text{b}}^{\text{av}}\left(1 - \text{e}^{-\lambda_{\text{b}}^{i=t_1, t_1+1, \ldots t_2}}\right)\right\} - \lambda_{\text{pv}}^{i}\right\} \\ &\quad \text{for} \quad \mathcal{S}_{\mathbb{P}}^{t} > \mathfrak{D}_{\mathbb{D}}^{t}, \mathfrak{S}_{\mathbb{P}}^{t} > \mathfrak{S}_{d}^{t} \end{aligned} \tag{31}$$

For $\mathcal{S}_{\mathbb{P}}^{t} < \mathfrak{D}_{\mathbb{D}}^{t}$ or $\mathfrak{S}_{\mathbb{P}}^{t} < \mathfrak{S}_{d}^{t}$, the EV will charge up to $\mathcal{S}_4$, and constraints as follows:

$$\lambda_{\text{ev}}^{i} = \mathcal{S}_4 \text{ and } \mathcal{S}_4 \leq 100\% \text{ of SOC} \tag{32}$$

3.1 Modified operation state

The power provided by the storages to minimise the peak load is given as

$$\begin{aligned} \mathcal{S}_{\mathbb{P}}^{s} = \Bigg\{ & \left\{\lambda_{\text{ev}}^{\text{av}}\left(1 - \text{e}^{-\lambda_{\text{ev}}^{i=t_1, t_1+1, \ldots, t_2}}\right)\right\} \\ & + \left\{\lambda_{\text{b}}^{\text{av}}\left(1 - \text{e}^{-\lambda_{\text{b}}^{i=t_1, t_1+1, \ldots t_2}}\right)\right\} + \lambda_{\text{pv}}^{i} \Bigg\} * \sum_{t=t_r^1}^{t_r^t} \cup \end{aligned} \tag{33}$$

where $\cup$ is a discrete random number with a function of time constant (t), and $\left(t_r^1 \leq t \leq t_r^t\right)$. This $\cup$ holds the discharging operation for a random time. The available grid power $\left(\mathcal{S}_{\mathbb{P}}^{c}\right)$ to charge the battery and EV is

$$\begin{aligned} \mathcal{S}_{\mathbb{P}}^{c} = \Bigg\{ & \left\{\lambda_{\text{ev}}^{\text{r}}\left(\text{e}^{(1/(-\lambda_{\text{ev}}^{i=t_1, t_1+1, \ldots, t_2)})}\right)\right\} \\ & + \left\{\lambda_{\text{b}}^{\text{r}}\left(\text{e}^{(1/(-\lambda_{\text{b}}^{i=t_1, t_1+1, \ldots t_2)})}\right)\right\} \Bigg\} * \sum_{t=t_r^1}^{t_r^t} \cup \\ & \text{for } \mathcal{S}_{\mathbb{P}}^{t} < \mathfrak{D}_{\mathbb{D}}^{t}, \mathfrak{S}_{\mathbb{P}}^{t} < \mathfrak{S}_{d}^{t} \end{aligned} \tag{34}$$

4 Case studies

Several case studies are carried out based on a real Australian household data [30]. Real weather data are also fed to the PV unit and weather-dependent household loads to get a real power generation and consumption, and also to investigate the

check: power demand $\mathcal{S}_{\mathcal{P}}^{t} = f\left(\mathcal{P}, t_{\ell}^{j}\right)$ and set the value $\mathcal{D}_{d}^{t}$

while $\left(\mathcal{S}_{\mathcal{P}}^{t} < \mathcal{D}_{d}^{t}\right)\{$

  calculate: the available power $\left(\mathcal{S}_{\mathcal{P}}^{c}\right)$ for battery storage and EV charging

  check: boundary conditions of battery storage $\lambda_{b}^{m}, \lambda_{b}^{l}, \lambda_{b}^{i}, \beta_{b}^{c}$ and calculate λ_{b}^{r}

  check: EV availability and its constraints $\lambda_{ev}^{m}, \lambda_{ev}^{l}, \lambda_{ev}^{i}, \beta_{ev}^{c}$ and calculate λ_{ev}^{r}

  check: PV output λ_{pv}^{i}

  while $\left(\lambda_{pv}^{i} > 0\right)\{$

    for $\left(\mathcal{S}_{\mathcal{P}}^{t} < \lambda_{pv}^{i}\right)\{$

      use the excess energy ξ_{ex}^{pv} to charge battery and EV$\}$

    for $\left(\mathcal{S}_{\mathcal{P}}^{t} > \lambda_{pv}^{i}\right)\{$

      take the extra power from grid$\}\}$

  while $\left(\lambda_{pv}^{i} = 0\right)\{$

    use the grid power $\mathcal{S}_{\mathcal{P}}^{c}$ for battery and EV charging$\}\}$

while $\left(\mathcal{S}_{\mathcal{P}}^{t} < \mathcal{D}_{d}^{t}\right)\{$

  calculate: the required load-support $\mathcal{S}_{\mathcal{P}}^{s}$

  Acquire: PV power output λ_{pv}^{i}

  if $\left(\lambda_{pv}^{i} > \mathcal{S}_{\mathcal{P}}^{s}\right)\{$

    $\lambda_{pv}^{i} \rightarrow \mathcal{S}_{\mathcal{P}}^{s}$

  elseif $\left(\lambda_{pv}^{i} < \mathcal{S}_{\mathcal{P}}^{s}\right)\{$

    check: boundary conditions of battery storage $\lambda_{b}^{m}, \lambda_{b}^{l}, \lambda_{b}^{i}, \beta_{b}^{c}$ and calculate λ_{b}^{r}

    check: EV availability and its constraints $\lambda_{ev}^{m}, \lambda_{ev}^{l}, \lambda_{ev}^{i}, \beta_{ev}^{c}$ and calculate λ_{ev}^{r}

    get the required power $\mathcal{S}_{\mathcal{P}}^{s}$ from EV and battery$\}$

  continue the process and check the step 2 and 14$\}$

Fig. 2 *Algorithm 1: load-based EMS*

performance of the EMS during uncertainty. The parameters considered in the case studies are listed in Table 1.

The considered microgrid consists of 16 houses, out of them 8 houses comprise of a roof-top PV unit (with a capacity of 1.5–2 kW), EVs, and BESSs. The capacity of the EV is considered 24 kWh, similar to that of a Nissan Leaf EV. It is assumed that the EV leaves home at 8 am and comes back at 4 pm, with no charging facility at work. The driving range is in between 15 and 25 km.

4.1 Load behaviour with and without PV

Domestic load curve in a particular weather and geographical location follows a similar pattern; however, the power demand for every household at that particular time might not be the same. The main aim of this case study is to analyse the impact of integrating PV units in the domestic system on its load behaviours. For example, Fig. 5*a* shows the load curve for nine different houses in a particular location for five days. The PV output with fluctuations is shown in Fig. 5*b*. Although the simulation output is shown in minute scale, the controller read the signal in a sub-second time scale. The hour-scale PV power fluctuation in Fig. 5*b* is shown as the second scale in Fig. 5*c*.

Fig. 5*d* shows the load curve of the houses with and without PVs and impact of the fluctuating PV power generation due to a fast-moving cloud. It is clear from the figure that PV power fluctuations impel different load curves (highly dependent on roof-top PVs) to behave in the same way.

4.2 Load-based EMS and their identical behaviour

In this case study, the impact of load-based uncoordinated EMS is investigated. The constraints for load-based EMS are SOC charging–discharging limits of the battery, and EV, EV availability, EV trip plans, PV power generation and load demand. Based on these constraints, EV and battery charge management are scheduled between peak and off-peak hours to minimise the cost. Additionally, the excess power generation from the PV unit is utilised to charge the battery and EV. As load conditions (peak and

1: Initialization:
check: power demand $\mathcal{S}_{\mathcal{P}}^{t} = f(\mathcal{P}, t_{\ell}^{j})$
check: electricity price signal $\mathfrak{S}_{\mathcal{P}}^{t}$
determine: the off-peak and peak price periods from the reference $\mathfrak{S}_{d}^{t}$
2: **while** $(\mathfrak{S}_{\mathcal{P}}^{t} < \mathfrak{S}_{d}^{t})\{$
3: calculate: the available power $(\mathcal{S}_{\mathcal{P}}^{c})$ for battery storage and EV charging
4: check: boundary conditions of battery storage and EV $\lambda_{b}^{m}, \lambda_{b}^{l}, \lambda_{b}^{i}, \beta_{b}^{c}, \lambda_{ev}^{m}, \lambda_{ev}^{l}, \lambda_{ev}^{i}, \beta_{ev}^{c}$ and calculate $\lambda_{b}^{r}, \lambda_{ev}^{r}$
5: check: PV output λ_{pv}^{i}
6: **if** $(\lambda_{pv}^{i} > 0)\{$
7: **for** $(\mathcal{S}_{\mathcal{P}}^{t} < \lambda_{pv}^{i})\{$
8: use the excess energy ξ_{ex}^{pv} to charge battery and EV$\}$
9: **for** $(\mathcal{S}_{\mathcal{P}}^{t} > \lambda_{pv}^{i})\{$
10: take the extra power from grid$\}\}$
11: **elseif** $(\lambda_{pv}^{i} = 0)\{$
12: use the grid power $\mathcal{S}_{\mathcal{P}}^{c}$ for battery and EV charging$\}\}$
13: **while** $(\mathfrak{S}_{\mathcal{P}}^{t} > \mathfrak{S}_{d}^{t})\{$
14: calculate: the required load-support $\mathcal{S}_{\mathcal{P}}^{s}$
15: Acquire: PV power output λ_{pv}^{i}
16: **if** $(\lambda_{pv}^{i} > \mathcal{S}_{\mathcal{P}}^{s})\{$
17: $\lambda_{pv}^{i} \rightarrow \mathcal{S}_{\mathcal{P}}^{s}$
18: **elseif** $(\lambda_{pv}^{i} < \mathcal{S}_{\mathcal{P}}^{s})\{$
19: check: boundary conditions of battery storage and EV $\lambda_{b}^{m}, \lambda_{b}^{l}, \lambda_{b}^{i}, \beta_{b}^{c}, \lambda_{ev}^{m}, \lambda_{ev}^{l}, \lambda_{ev}^{i}, \beta_{ev}^{c}$ and calculate $\lambda_{b}^{r}, \lambda_{ev}^{r}$
20: get the required power $\mathcal{S}_{\mathcal{P}}^{s}$ from EV and battery$\}$
21: continue the process and check the step 2 and 13$\}$

Fig. 3 *Algorithm 2: price-based EMS*

off-peak load) are key parameters to determine the discharge and charge management, PV power fluctuations may lead the houses highly dependent on roof-top PV units to switch between peak and off-peak states rapidly. Therefore, storages (EVs and stationary battery) are also switched between charging and discharging modes rapidly. The rebound effect by this storage may create big spikes of power demand in the substation. As the load curves of every household under a substation are not identical, normal load fluctuation with PV penetration has less impact to the grid, as shown in Fig. 6. It is because household load does not fluctuate drastically like PV fluctuations due to shading by trees or fast-moving clouds. Moreover, the rebound effect occurs randomly by various EMS which has less significance at the substation.

In this investigation, for some houses 40–85% day-time off-peak power demand is met by the roof-top PVs. Therefore, any

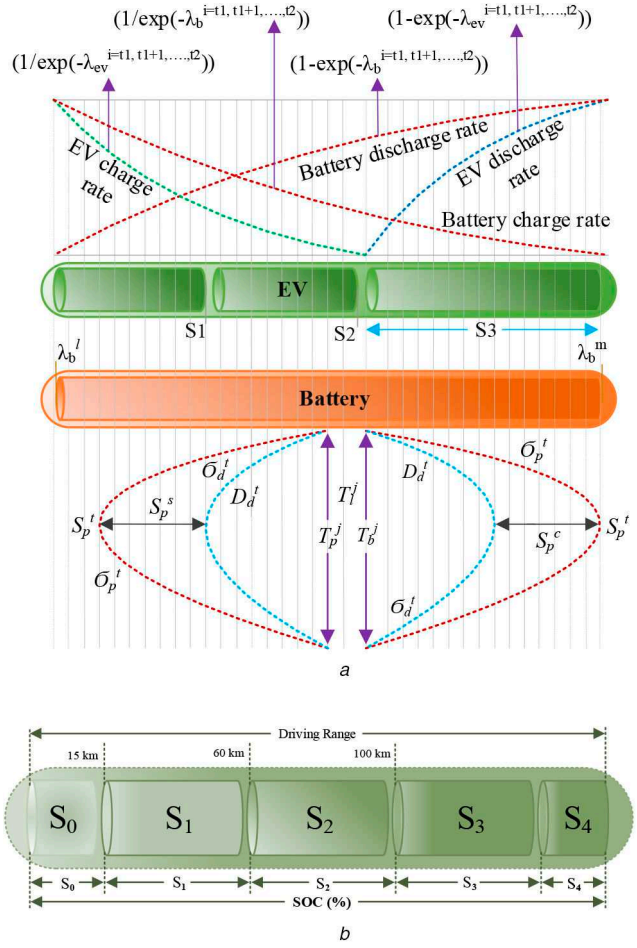

Fig. 4 *Charging-discharging management of EV and battery storage [5, 25]*
(a) EV and battery charging–discharging constraints, ***(b)*** EV battery SOC segmentation and management

Table 1 Component specification used in the simulation

Component	Value
no. of houses	16
no. of houses that uses a EMS	8
PV capacity	1.5–2 kW
battery capacity	2.5–5 kWh
EV capacity	24 kWh
battery charge–discharge constraints λ_{b}^{l}, λ_{b}^{m}	40%, 98%
EV charge–discharge constraints S_0, S_1, S_2, S_3, S_4	10, 25, 50, 85, 95% SOC
EV trip plan	8 am to 4 pm, random 15–25 km distance

fluctuations in PV output power has a significant impact on load curve as shown in Fig. 7. Moreover, these load-curve fluctuations are also experienced by all the houses comprising of roof-top PV units. In this case, load-based EMS of these houses also experiences operational state fluctuations at the same time. In this case study, eight houses use the same load-based EMS (eight houses do not have an EMS) and experiences operation mode fluctuations due to PV power fluctuations at the same time. Since the rebound effect occurs at the same time due to load-curve

$$\alpha(t) = \underbrace{\left\{\lambda_{\text{ev}}^{r}\left(\text{e}^{(1/(-\lambda_{\text{ev}}^{i=t_1,t_1+1,\ldots,t_2}))}\right)\right\}} = \left\{\mathcal{S}_{\mathbb{P}}^{c} - \lambda_{\text{b}}^{r}\left(\text{e}^{(1/(-\lambda_{\text{b}}^{i=t_1,t_1+1,\ldots,t_2}))}\right)\right\} \quad (30)$$

$$\text{for} \quad \mathcal{S}_1 < \lambda_{\text{ev}}^{i} < \mathcal{S}_3, \mathcal{S}_{\mathbb{P}}^{t} < \mathfrak{D}_{\mathbb{D}}^{t}, \mathfrak{S}_{\mathbb{P}}^{t} < \mathfrak{S}_{d}^{t}$$

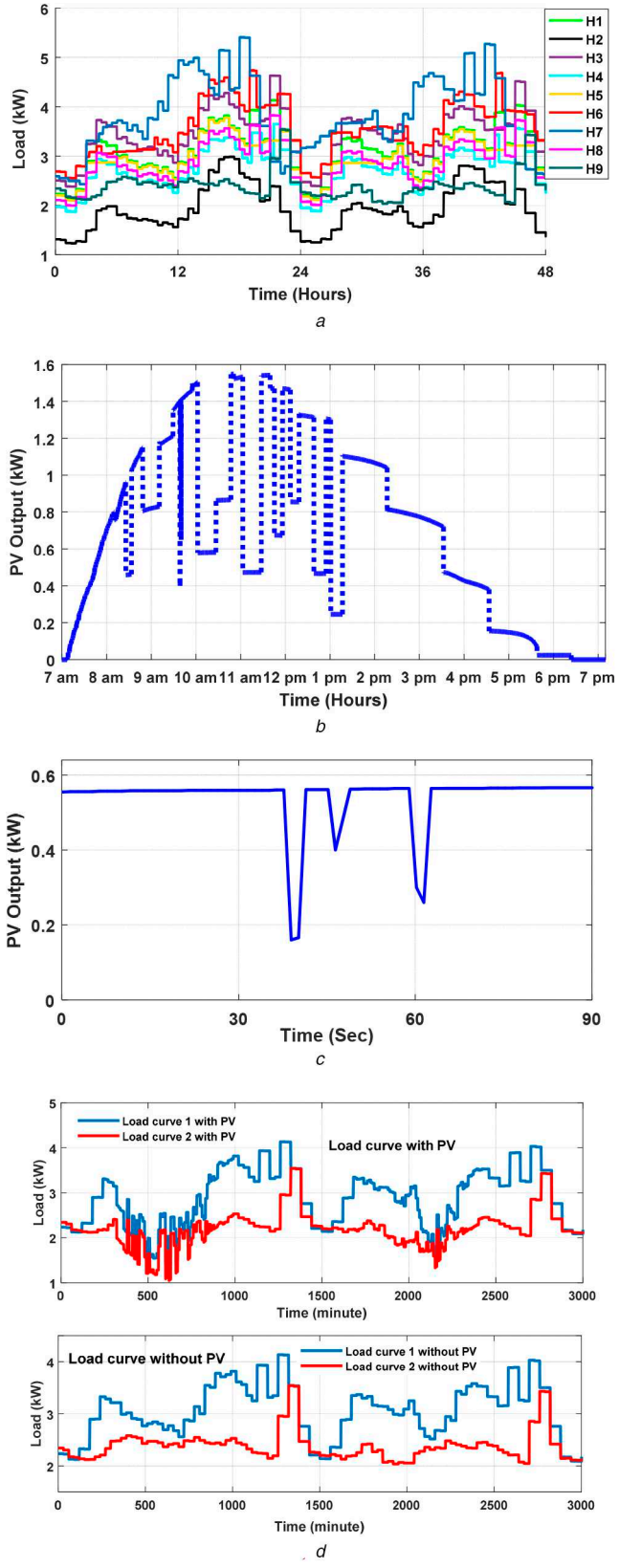

Fig. 5 *Domestic load curve and the impact of controlled and uncontrolled PV power on it*

(a) Load curve of the houses, 'H1 = Home-1, …, H9 = Home-9', ***(b)*** PV power output (fluctuation case), ***(c)*** PV output considered to the controller decision making in the second scale, ***(d)*** Load curve with and without PV integration

similarity, the summation of rebound effect by individual EMS creates big spikes of power demand at the substation.

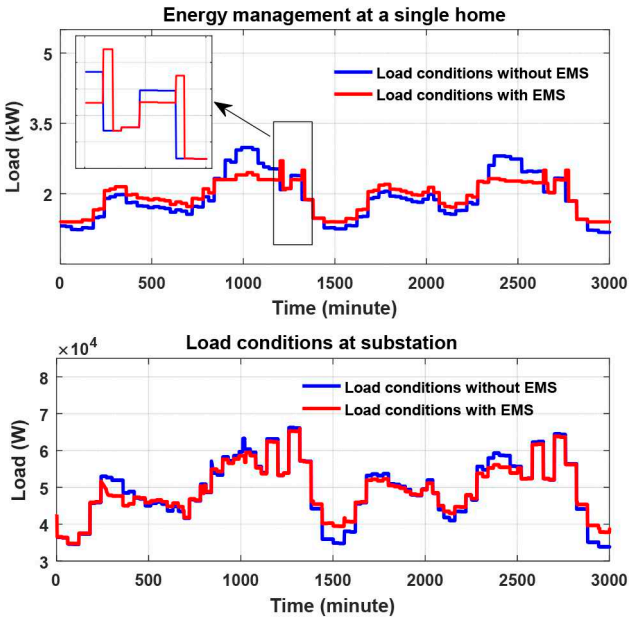

Fig. 6 *EMS at a single home and its impact at substation when PVs are not connected*

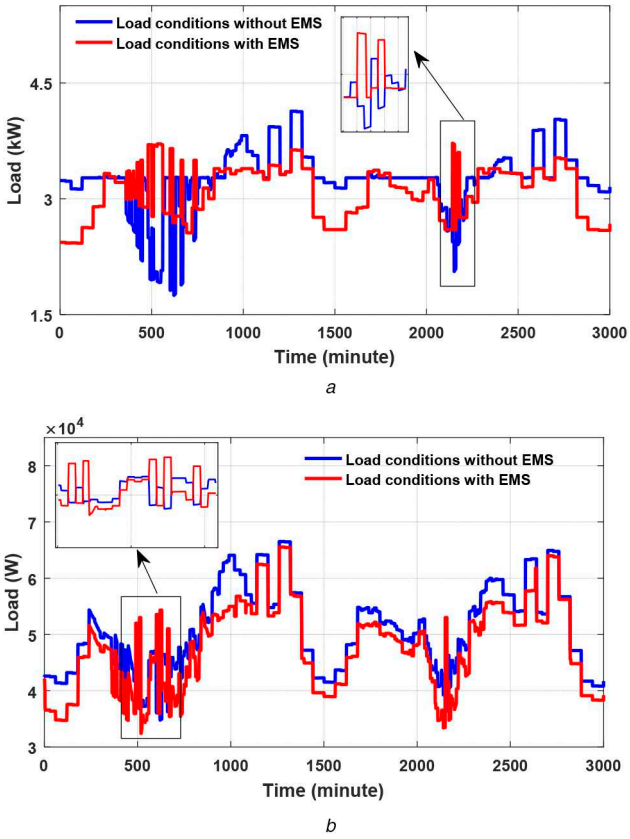

Fig. 7 *EMS performance considering PV power generation charateristics*

(a) Load conditions with and without EMS at a single home when PV is connected, ***(b)*** Load conditions with and without EMS at the substation when PV is connected

4.3 Price-based EMS and their identical behaviour

In this case study, price-based EMS are tested and their impacts on the grid in an uncoordinated state are investigated. The price-based EMS also has similar constraints like load-based EMS. However, unlike load-based EMS, price-based EMS follows electricity price to manage charging–discharging of the EVs and battery storages, to minimise cost. In this case, price-based EMS are deployed in eight houses, and their impacts on an individual house and at substation are investigated, as shown in Figs. 8*a–c*. The EMS responses based on the electricity price are shown in Fig. 8*b*. Any fluctuations in

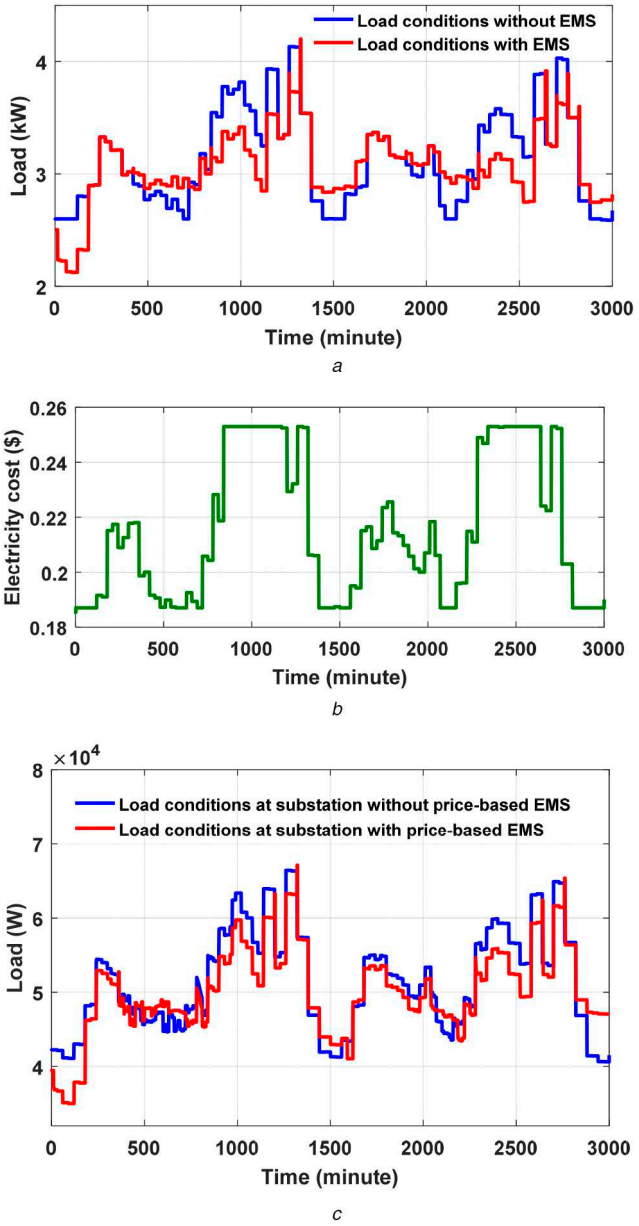

Fig. 8 *Perofrmance analysis of price-based EMS*
(a) Load conditions with and without price-based EMS at a single home, ***(b)*** Electricity costs, ***(c)*** Load conditions with and without price-based EMS at the substation

the electricity prices result in a fluctuation of the operation state of the EMS. Since all the EMS are working based on the same algorithm and same price signal, any rebound effect due to price fluctuation may create EMS fluctuation at the same time. As a result, substation faces big power demand spikes in their load curves.

4.4 Impact minimisation: locking and randomisation

Proper coordination among uncoordinated EMS could be a solution to minimise the rebound and oscillation impact. However, it requires communication arrangements and advanced coordinated control devices. In this study, a simple solution that does not require coordination among EMS and control devices is proposed. A novel locking and randomisation method is introduced. In this approach, a time constant is added with the charging–discharging scheduling of the battery and EVs, as shown in (33) and (34). This time constant will lock the operation for both price-based and load-based EMS. Thus, the operation mode fluctuation will not occur based on the PV-power generation fluctuations. Additionally, the value of this time constant (locking-time) is randomly assigned among EMS. As a result, every EMS have their own time constant

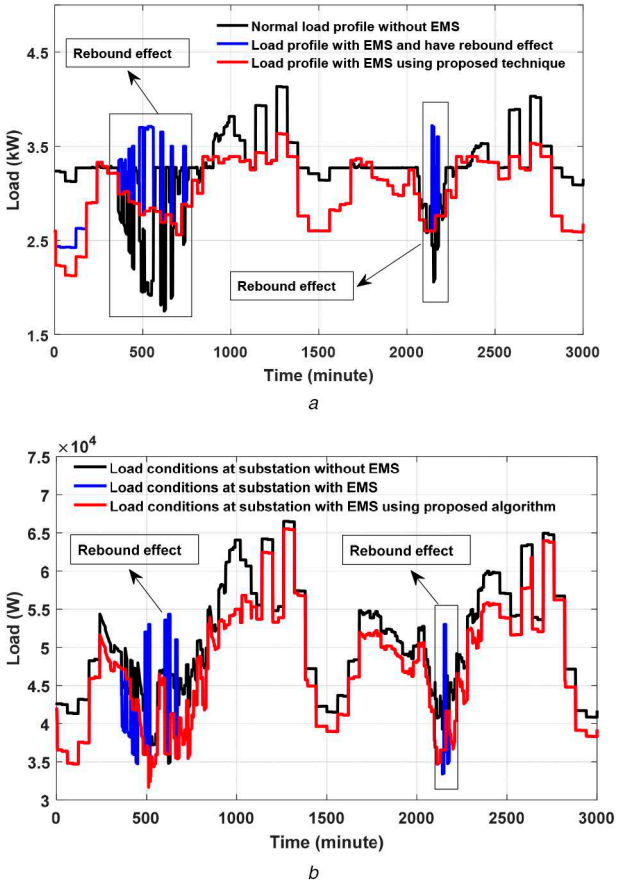

Fig. 9 *Load conditions with and without price-based EMS, and locking and randomisation are enabled*
(a) Load conditions at home, ***(b)*** Load conditions at substation

and get a different reference value to operate and respond to the changes in load and electricity price. For example, after introducing this technique, the combined response from PV, EV, and battery to shave the peak $(\mathcal{S}^s_{\mathbb{P}})$ for every house now get a different reference point to operate, e.g. $\{(\mathcal{S}^s_{\mathbb{P}}) * \cup^1_{t_r}\}, \{(\mathcal{S}^s_{\mathbb{P}}) * \cup^2_{t_r}\}, \ldots, \{(\mathcal{S}^s_{\mathbb{P}}) * \cup^t_{t_r}\}$. Likewise, different houses and their charging reference points also become different, i.e. $\{(\mathcal{S}^c_{\mathbb{P}}) * \cup^1_{t_r}\}, \{(\mathcal{S}^c_{\mathbb{P}}) * \cup^2_{t_r}\}, \ldots, \{(\mathcal{S}^c_{\mathbb{P}}) * \cup^t_{t_r}\}$. So, the overall impact of the rebound effects by the EMS decreases at the substation.

The eight houses that were using EMS are now operating under the proposed random time constant and locking systems, as shown in Fig. 9. Fig. 9*a* shows the impact of the proposed approach to a single house, and Fig. 9*b* shows their impact at the substation. Fig. 9*a* shows that the use of uncoordinated EMS minimises the peak load; however, during renewable energy fluctuation cases, the rebound effect creates oscillation and peak spikes immediately after the peak conditions. It is because, after the peak conditions when off-peak hours occur, all the storages and EVs start charging. As the proposed locking and randomisation process delays the EMS activation randomly, the load profile does not give any peak spikes and oscillations. As the renewable energy output in a specific geographical location shows similar pattern due to the same weather conditions, any power generation fluctuations at the customers' points provide impact at the substation. Fig. 9*b* shows the impact of uncoordinated EMS having rebound behaviour at the substation and the improvement of oscillations after using the proposed system.

A summary of the goal and findings of the paper is summarised in the paper and compared with the previous studies in Table 2.

5 Conclusion

The main goal of the research was to investigate the impact of uncoordinated EMS having rebound effect in a microgrid and

Table 2 Summary of the goals and findings of the paper compared to the previous studies

Previous studies	This study
[17] • It investigates the scenarios under which the rebound effect can lead to instability in terms of the area control error (ACE) [17]. • The findings of this study show that under normal circumstances the rebound effect has positive impact on the ACE. However, in some worst-case scenario, the rebound effect may create oscillations in the ACE, which may lead to an unstable system [17].	• It investigates the impact of uncoordinated EMS having rebound effect in a small-microgrid and provide a feasible solution to mitigate their unwanted effects • The rebound effect in islanded small-microgrid under price and load-based EMS due to quick fluctuations in prices and PV power generation may create spikes in the load demand curve. • For a large network or grid-connected systems or slow change of prices and PV power generation, the rebound effect may be trivial.
[18] • The study investigates the rebound effects of demand response and its behaviour during frequency restoration. • It shows that in some extreme cases, the rebound effects can lead to oscillations in the power systems [18].	
[19] • The study analyses the performance of a demand response (DR) system, installed in the Hartley Bay, British Columbia, to reduce the fuel consumption during peak load periods [19]. • It finds that the DR systems reduces peak demand significantly, however, a significant rebound peak occurs following each event [19].	

provide a feasible solution to mitigate their unwanted effects. Two different types of EMS are modelled and tested to observe their behaviours under load variations. This study has shown that for a highly PV-penetrated small grid, fluctuations due to fast-moving clouds result in a similar pattern of fluctuations in various load curves. The rebound effect by EMS due to this fluctuation creates large peaks to the grid. Likewise, if all the EMS work based on the same algorithm and same price signal, any rebound effect due to price fluctuation may create fluctuations in EMS response at the same time resulting in a high peak at the substation. The study has found that the addition of a time lock and its randomisation, minimises this effect. This rebound effect maybe trivial in case of the grid-connected systems or in large networks, or if the load, price and PV power generation fluctuations occur slowly. The future research could also be conducted to investigate the effectiveness of the proposed technique to a grid-connected system, with a wind power generation fluctuation case.

6 References

[1] Elamin, W.E., Shaaban, M.F.: 'New real-time demand-side management approach for energy management systems', *IET Smart Grid*, 2019, **2**, pp. 183–191

[2] Ampofo, D.O., Al-Hinai, A., El Moursi, M.: 'Active distribution network with efficient utilisation of distributed generation ancillary', *IET Smart Grid*, 2018, **1**, (4), pp. 151–158

[3] Teo, T.T., Logenthiran, T., Woo, W.L., *et al.*: 'Advanced control strategy for an energy storage system in a grid-connected microgrid with renewable energy generation', *IET Smart Grid*, 2018, **1**, (3), pp. 96–103

[4] Ioakimidis, C.S., Thomas, D., Rycerski, P., *et al.*: 'Peak shaving and valley filling of power consumption profile in non-residential buildings using an electric vehicle parking lot', *Energy*, 2018, **148**, pp. 148–158

[5] Mahmud, K., Hossain, M.J., Town, G.E.: 'Peak-load reduction by coordinated response of photovoltaics, battery storage, and electric vehicles', *IEEE Access*, 2018, **6**, pp. 29353–29365

[6] Sehar, F., Pipattanasomporn, M., Rahman, S.: 'An energy management model to study energy and peak power savings from PV and storage in demand responsive buildings', *Appl. Energy*, 2016, **173**, pp. 406–417

[7] Mahmud, K., Hossain, M.J., Ravishankar, J.: 'Peak-load management in commercial systems with electric vehicles', *IEEE Syst. J.*, 2018, **12**, (2), pp. 1872–1882

[8] Sehar, F., Pipattanasomporn, M., Rahman, S.: 'Demand management to mitigate impacts of plug-in electric vehicle fast charge in buildings with renewables', *Energy*, 2017, **120**, pp. 642–651

[9] Roselli, C., Sasso, M.: 'Integration between electric vehicle charging and PV system to increase self-consumption of an office application', *Energy Convers. Manage.*, 2016, **130**, pp. 130–140

[10] Nie, Y., Wang, X., Cheng, K.W.E.: 'Multi-area self-adaptive pricing control in smart city with EV user participation', *IEEE Trans. Intell. Transp. Syst.*, 2017, **19**, (7), pp. 2156–2164

[11] Ma, K., Wang, C., Yang, J., *et al.*: 'Energy management based on demand-side pricing: a supermodular game approach', *IEEE Access*, 2017, **5**, pp. 18219–18228

[12] Hayes, B., Melatti, I., Mancini, T., *et al.*: 'Residential demand management using individualized demand aware price policies', *IEEE Trans. Smart Grid*, 2017, **8**, (3), pp. 1284–1294

[13] Alam, M.J.E., Muttaqi, K.M., Sutanto, D.: 'Effective utilization of available PEV battery capacity for mitigation of solar PV impact and grid support with integrated V2G functionality', *IEEE Trans. Smart Grid*, 2016, **7**, (3), pp. 1562–1571

[14] Luthander, R., Widén, J., Munkhammar, J., *et al.*: 'Self-consumption enhancement and peak shaving of residential photovoltaics using storage and curtailment', *Energy*, 2016, **112**, pp. 221–231

[15] Yang, Y., Li, H., Aichhorn, A., *et al.*: 'Sizing strategy of distributed battery storage system with high penetration of photovoltaic for voltage regulation and peak load shaving', *IEEE Trans. Smart Grid*, 2014, **5**, (2), pp. 982–991

[16] Brenna, M., Foiadelli, F., Longo, M.: 'The exploitation of vehicle-to-grid function for power quality improvement in a smart grid', *IEEE Trans. Intell. Transp. Syst.*, 2014, **15**, (5), pp. 2169–2177

[17] Lütolf, P.: 'Impact of the rebound effect of demand response on secondary frequency control'. Master's thesis, ETH Zürich, 2016

[18] Lütolf, P., Scherer, M., Mégel, O., *et al.*: 'Rebound effects of demand-response management for frequency restoration'. 2018 IEEE Int. Energy Conf. (ENERGYCON), Limassol, Cyprus, 2018, pp. 1–6

[19] Wrinch, M., Dennis, G., EL-Fouly, T.H.M., *et al.*: 'Demand response implementation for improved system efficiency in remote communities'. 2012 IEEE Electrical Power and Energy Conf., London, ON, Canada, 2012, pp. 105–110

[20] Reihani, E., Sepasi, S., Roose, L.R., *et al.*: 'Energy management at the distribution grid using a battery energy storage system (BESS)', *Int. J. Electr. Power Energy Syst.*, 2016, **77**, pp. 337–344

[21] Erdinc, O., Paterakis, N.G., Mendes, T.D.P., *et al.*: 'Smart household operation considering bi-directional EV and ESS utilization by real-time pricing-based DR', *IEEE Trans. Smart Grid*, 2015, **6**, (3), pp. 1281–1291

[22] Igualada, L., Corchero, C., Cruz-Zambrano, M., *et al.*: 'Optimal energy management for a residential microgrid including a vehicle-to-grid system', *IEEE Trans. Smart Grid*, 2014, **5**, (4), pp. 2163–2172

[23] Xu, Q., Ding, Y., Yan, Q., *et al.*: 'Day-ahead load peak shedding/shifting scheme based on potential load values utilization: theory and practice of policy-driven demand response in China', *IEEE Access*, 2017, **5**, pp. 22892–22901

[24] Arun, S.L., Selvan, M.P.: 'Dynamic demand response in smart buildings using an intelligent residential load management system', *IET Gener. Transm. Distrib.*, 2017, **11**, (17), pp. 4348–4357

[25] Mahmud, K., Rahman, M.S., Ravishankar, J., *et al.*: 'Real-time load and ancillary support for a remote island power system using electric boats', *IEEE Trans. Ind. Inf.*, 2019, pp. 1–1

[26] Khan, K.H., Ryan, C., Abebe, E.: 'Day ahead scheduling to optimize industrial HVAC energy cost based ON peak/OFF-peak tariff and weather forecasting', *IEEE Access*, 2017, **5**, pp. 21684–21693

[27] Malik, S.M., Ai, X., Sun, Y., *et al.*: 'Voltage and frequency control strategies of hybrid AC/DC microgrid: a review', *IET Gener. Transm. Distrib.*, 2017, **11**, (2), pp. 303–313

[28] Sowmmiya, U., Govindarajan, U.: 'Control and power transfer operation of WRIG-based WECS in a hybrid AC/DC microgrid', *IET Renew. Power Gener.*, 2018, **12**, (3), pp. 359–373

[29] Sharma, R.K., Mishra, S.: 'Dynamic power management and control of a PV PEM fuel-cell-based standalone AC/DC microgrid using hybrid energy storage', *IEEE Trans. Ind. Appl.*, 2018, **54**, (1), pp. 526–538

[30] 'Electricity Price and Demand'. Available at https://aemo.com.au/Electricity/National-Electricity-Market-NEM/Data-dashboard, accessed May 2018

[31] El-Shimy, M., Sharaf, A., Khairy, H., *et al.*: 'Reduced-order modelling of solar-PV generators for small-signal stability assessment of power systems and estimation of maximum penetration levels', *IET Gener. Transm. Distrib.*, 2018, **12**, (8), pp. 1838–1847